

Electronic properties of transition-metal dichalcogenides

Agnieszka Kuc, Thomas Heine, and Andras Kis

Graphene is not the only prominent example of two-dimensional (2D) materials. Due to their interesting combination of high mechanical strength and optical transparency, direct bandgap and atomic scale thickness transition-metal dichalcogenides (TMDCs) are an example of other materials that are now vying for the attention of the materials research community. In this article, the current state of quantum-theoretical calculations of the electronic and mechanical properties of semiconducting TMDC materials are presented. In particular, the intriguing interplay between external parameters (electric field, strain) and band structure, as well as the basic properties of heterostructures formed by vertical stacking of different 2D TMDCs are reviewed. Electrical measurements of MoS_2 , WS_2 , and WSe_2 and their heterostructures, starting from simple field-effect transistors to more demanding logic circuits, high-frequency transistors, and memory devices, are also presented.

Introduction

After quantum dots, nanowires, and nanotubes, two-dimensional (2D) materials in the form of sheets with atomic-scale thickness represent the most recent nanoscale material family under intense study. These materials appear in their bulk form as stacks of layers held together via van der Waals interaction in crystals. Single layers with atomic-scale thickness can be extracted from such crystals. The best-known example is graphite, composed of individual graphene layers. Two-dimensional materials are attractive for use in electronic devices because, compared to nanowires and nanotubes, it is easier to fabricate complex structures from them. Their atomic-scale thickness makes it possible to tune their properties using external electric fields, while control over the number of layers in mesoscopic structures gives an additional way to modify their electronic and optical properties.^{1,2}

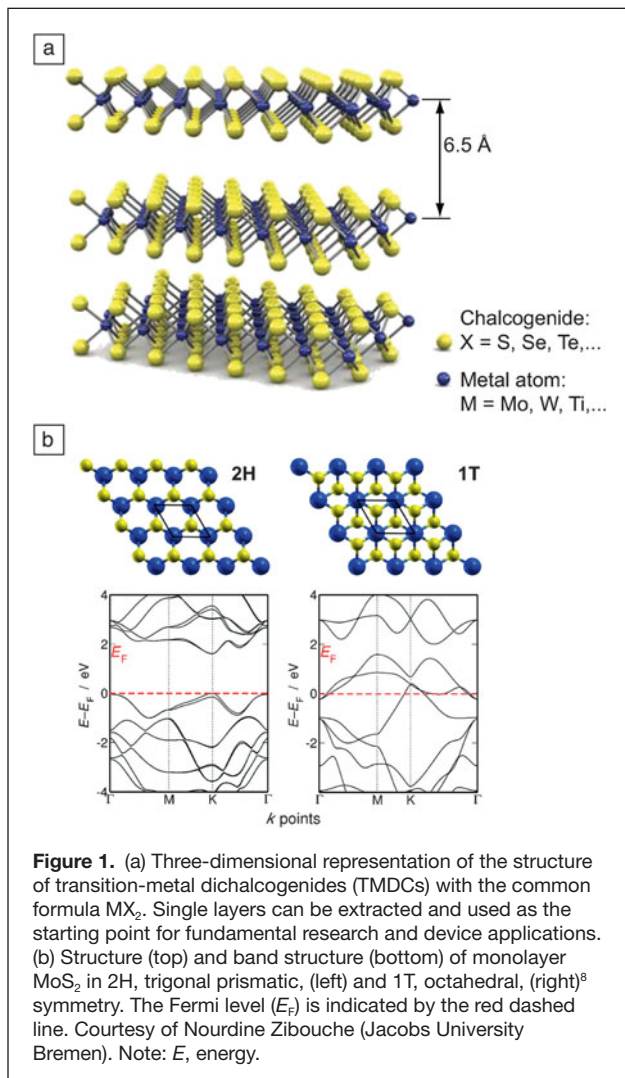
The first layered material to be thinned to a single monolayer (ML) was graphite, where the ML is referred to as graphene.³ It continues to be widely studied because of its rich physics and high mobility.⁴ However, pristine graphene does not have a bandgap, which is required for many applications in electronics and optoelectronics. Bandgaps can be engineered in graphene, but this increases complexity either reduces mobilities to the level of strained silicon films ($\sim 100 \text{ cm}^2/\text{Vs}$ at room temperature) or requires voltages on the order of 100 V.^{5,6}

One of the key advances that brought attention to 2D semiconductors was the demonstration of a field-effect transistor (FET) with a high ON/OFF ratio based on a single layer of MoS_2 ,⁷ a semiconducting material from the transition-metal dichalcogenide (TMDC) family. This was the first demonstration of a high-quality device based on a 2D material other than graphene.

MoS_2 (**Figure 1**) is a member of a large family of materials known as TMDCs (please see the Introduction article in this issue of *MRS Bulletin*). They have the common chemical formula MX_2 , where M stands for a transition metal ($\text{M} = \text{Mo}, \text{W}, \text{Nb}, \text{Ta}, \text{Ti}, \text{Re}$) and X for Se, S, or Te. Bulk TMDC crystals are formed by vertical stacking of 2D layers that are $\sim 6.5 \text{ \AA}$ thick. Depending on the chemical composition, they can have different electrical properties ranging from semiconducting to superconducting. Single layers can be extracted using the micromechanical cleavage technique,^{9,10} commonly used for the production of graphene or liquid phase exfoliation, a mild solvent-based exfoliation technique.¹¹ Large-area MoS_2 can be grown using chemical-vapor-deposition-like growth techniques.^{12,13} The lack of dangling bonds also makes it possible to re-stack different 2D materials in the vertical direction and produce heterostructures¹⁴ without the requirement of lattice matching.

Around 60 TMDC materials were known in the late 1960s, with around 40 of them having a layered structure¹⁵ (**Table I**).

Agnieszka Kuc, Jacobs University Bremen, Germany; a.kuc@jacobs-university.de
Thomas Heine, Jacobs University Bremen, Germany; t.heine@jacobs-university.de
Andras Kis, École Polytechnique Fédérale de Lausanne, Switzerland; andras.kis@epfl.ch
DOI: 10.1557/mrs.2015.143



First reports of ultrathin (10 nm thick) MoS₂ date back to 1963,¹⁶ while the production of single-layer MoS₂ in suspension was first reported in 1986.¹⁷ The rapid growth of graphene-related research and the development of new techniques for working with ultrathin layered materials opened new perspectives for the study of 2D TMDC layers. The indication that TMDC MLs are fundamentally different from thicker bulk material came with the realization that the bandgap of MoS₂ changes from the bulk value of 1.2 eV¹⁸ to 1.8 eV^{19,20} as the thickness is decreased down to a ML. This is due to quantum-mechanical confinement in the vertical direction²¹ and the resulting change in hybridization in orbitals related to M and X atoms. Moreover, unlike the bulk material, single-layer MoS₂ is a direct gap semiconductor. This seems to be a general feature shared by many other semiconducting TMDCs (MoSe₂, WS₂, WSe₂, MoTe₂) that are expected to show indirect to direct bandgap transitions in the limit of a single layer, spanning the 1.1–1.9 eV bandgap energy range.^{21–25}

Even though a large number of layered TMDCs are known, only a handful of them are widely available in the form of

a synthetic material. Most of the recent research efforts are concentrated on semiconducting TMDCs due to their potential for applications in electronics, with MoS₂ being the most studied example due to the fact that it is also available in the form of a naturally occurring mineral, molybdenite.²⁶

Modeling the electronic structure of TMDCs

Important contributions to the development of the field of 2D crystals have come from theory. While theory offers an explanation of many fundamental experimental effects, many phenomena have been predicted by computer simulations. In the following, some of these examples are compiled, with a focus on our own contributions. It is important to note that calculations on 2D materials may require different approaches and computational details, so the interested reader is referred to our recent tutorial reviews of the topic.^{1,36}

Theoretical modeling offers fast screening of many 2D crystals. We have compiled the structural and electronic properties of a large selection of 2D crystals, thus providing a database of bandgaps, effective electron and hole masses, lattice parameters, and band structures for further investigation by experiment and theory.³⁷ Materials with spectacular properties invite further investigation; for example, in the case of PdS₂, a Group 10 TMDC with 1T symmetry is semiconducting as a ML, but becomes semimetallic as a bilayer (BL).³⁸

When Group 6 semiconducting $-MX_2$ materials with the 2H (trigonal prismatic) structure type (Figure 1b) are confined from the bulk to the ML, their crystal symmetry lowers, and their electronic structure changes significantly. An important example of this quantum confinement is the observed enhanced photoluminescence signal from a MoS₂ ML, which has been rationalized by band structure calculations.^{19,20} MoS₂, when thinned down to a ML, undergoes an indirect to direct bandgap transition, as illustrated in **Figure 2**. We have shown that this phenomenon is not restricted to MoS₂ but is also present in other Group 6 MX₂ materials.²¹

Figure 2 also shows the importance of relativistic effects. Schwingenschlögl et al.³⁹ predicted giant spin-orbit (SO) splitting for MoS₂ ML on the basis of density functional theory calculations. This strong quantum effect alters the electronic levels of the material, depending on their spin signature, due to the interaction of the intrinsic electron spin with its angular orbital momentum. This effect is also general for all 2H Group 6 MX₂ materials, with values reaching 480 meV for WTe₂.⁴⁰

It is intriguing to compare the electronic property changes of MX₂ MLs and BLs. While MLs show giant SO splittings, these are absent in the bulk and BLs, which is explained by the presence of an inversion center, resulting in the presence of two degenerate orbitals of opposite spin for any point in the band structure. Thus, it is possible to exploit the symmetry for tuning the SO splitting, offering interesting materials for spintronic applications. Any symmetry breaking will introduce SO splitting in the BL. One way to do this is by an external electric field normal to the basal plane, for example, provided

Table I. Overview of stable layered transition-metal dichalcogenides.

Electrical Property	Material	Possible Role in Electronic Devices
Metallic	NbSe₂ , ²⁷ NbS ₂ , NbTe ₂	Interconnects, Josephson junctions, superconducting qubits
	TaS₂ , TaSe ₂ , TaTe ₂	
	ScS ₂ , ScSe ₂ , ScTe ₂	
	TiS ₂ , TiSe ₂ , TiTe ₂	
	VS₂ , VSe ₂ , VTe ₂	
	MnS ₂ , MnSe ₂ , MnTe ₂	
	FeS₂ , FeSe ₂ , FeTe ₂	
	NiTe ₂	
Semimetallic	TiSe ₂ , WTe₂ ²⁸	Interconnects
Semiconducting	MoS₂ , ⁸ MoSe₂ , ²⁹ MoTe₂	Transistors, switches, sensors, optoelectronic devices
	WS₂ , ³⁰ WSe₂ ^{31,32}	
	CrS ₂ , CrSe ₂ , CrTe ₂	
	NiS ₂ , NiSe ₂	
	ZrS ₂ , PdS ₂ ³³	
	ReS₂ , ³⁴ ReSe₂ , ³⁵ ReTe ₂	
	HfS₂	

First experimental studies on mesoscopic structures have been performed on compounds in bold. 2H (trigonal prismatic) structure; most stable are in red.²⁵

by a gate voltage, as shown in **Figure 3**. This introduces a Stark effect—the applied electric field quasi-linearly splits the bands—and the SO splitting converges quickly to about the same values as found for the respective MLs.⁴¹ After a field strength of ~ 5 V/nm, a value that can be reached experimentally, the SO splitting is saturated. However, MX₂ MLs

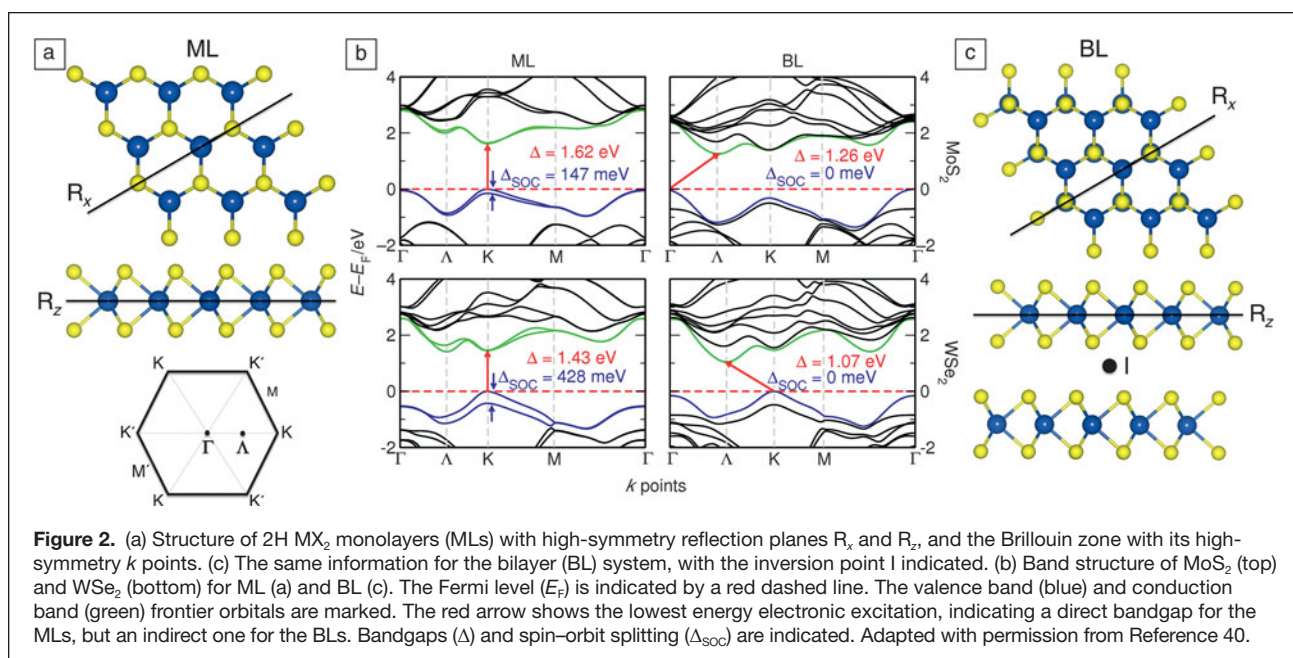
are insensitive to the presence of even strong gate voltages.⁴²

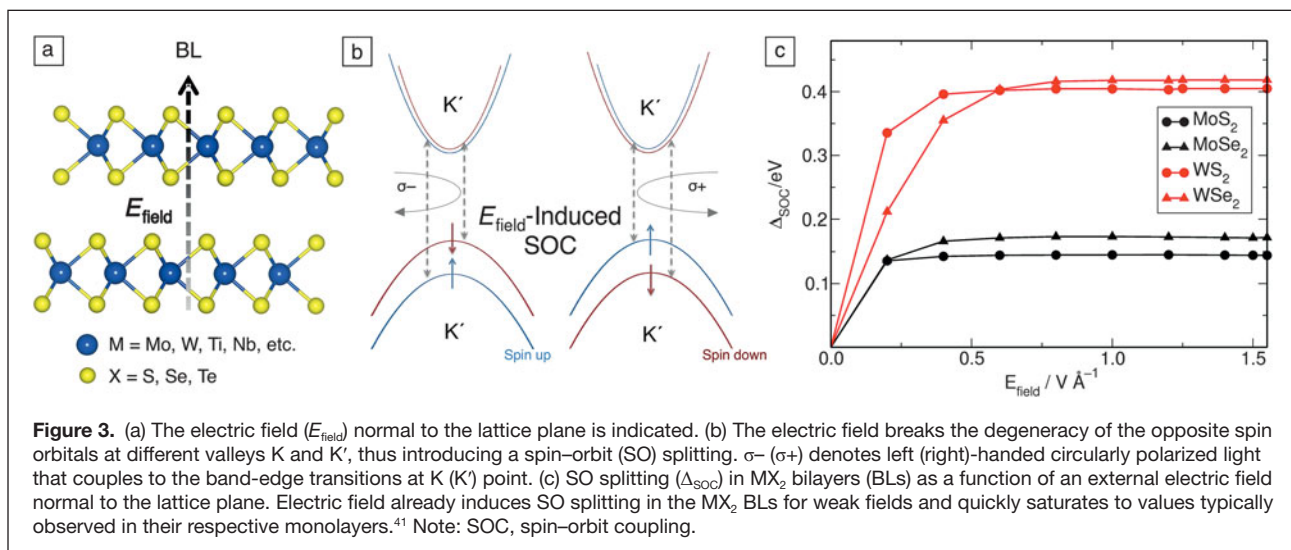
External fields have another important effect on the electronic structure of MX₂ materials and can be used to tune the bandgap. Again, MLs are almost unaffected by external electric fields, with bandgap and effective electron and hole masses remaining stable.⁴² Only at very high fields of about 50 V/nm do the bandgaps get smaller and eventually vanish, but at such a high field strength in the laboratory, MLs would not remain intact. BLs show a quasi-linear decrease in the bandgap in the presence of an external field (**Figure 4**).

Mechanical deformation is another way to change the electronic structure in MX₂ materials. Group 6 2H MX₂ materials readily form nanotubes and nanoribbons, which have been investigated for their tribological properties. WS₂ nanotubes resist strain for elongations of 10% and more, thereby showing a linear strain–stress relation up to rupture.⁴³ In the 2D crystal, deformation is accompanied by strong electronic effects (straintronics). Under isotropic and unidirectional strain,

the bandgap is almost linearly lowered until a semiconductor–metal transition is observed at about 10% isotropic strain (Figure 4).⁴⁴ Note that strained MoS₂ ML, as well as related Group 6 MX₂ MLs, are no longer direct bandgap semiconductors.

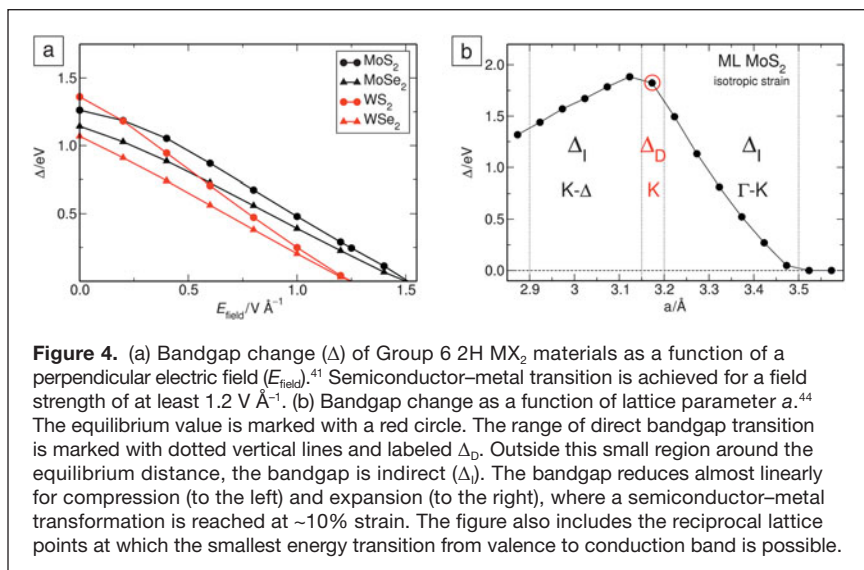
The metallic state has been confirmed by explicit calculations of the quantum conductance, indicating that transport





channels are opened. Unidirectional strain gives similar results but with a smaller magnitude. Also, unidirectional strain can be employed to introduce anisotropy to the electronic properties.⁴⁵ However, it is difficult to introduce strain experimentally. One way is to employ an atomic force microscope (AFM) tip; computer simulations of an indentation experiment showed that the electronic structure of MoS₂ remains remarkably stable up to the point of piercing by the tip.⁴⁶ Another method is bending, or thermal expansion, which could be carried out on a substrate with a strong thermal expansion coefficient. However, due to the low friction coefficient of Group 6 MX₂, only a small amount of isotropic strain or compression can be introduced into a MoS₂ ML.⁴⁷ Nevertheless, the first experiments with strain up to 2% confirm that the bandgap of MoS₂ ML can be tuned by strain with an accompanying bandgap decrease of ~70 meV per % strain.^{48,49}

The electronic properties of MX₂ materials are strongly affected by defects that often form due to the synthesis procedure. For instance, point defects lead to new photoemission peaks and enhanced photoluminescence intensity in MoS₂ MLs.⁵⁰ These effects can be attributed to the trapping potential of free charge carriers and to localized excitons. Simulations of the electronic structure of defective MoS₂ ML show that defects introduce mid-gap states that act as scattering centers.⁵¹ Our non-equilibrium Green's function transport simulations, where the current due to a potential drop between two leads in the presence of a bias voltage is calculated, show that single atomic vacancies can significantly reduce the average conductance and lead to significant anisotropy of electron transfer in MLs with grain boundaries. These results indicate that defects are important limiting factors in electronic transport,⁵² thus explaining a large variation of conductivity in different samples.



Similar to freestanding graphene, MX₂ MLs are not completely flat, which was shown from the microscopic structure of thin MoS₂ layers using high-resolution transmission electron microscopy and atomic force microscopy.⁵³ MoS₂ MLs form ripples, which may reach heights of 6–10 Å for a lateral flake length of 6–10 nm. This was supported by Born-Oppenheimer molecular dynamics simulations. Here, forces on the atoms are calculated from first principles, while the dynamics of the atoms is calculated using classical theory. These simulations confirmed that the inherent dynamics of MoS₂ MLs lead to spontaneous ripple formation even at temperatures as low as 77K.⁵⁴ The ripples converged to the heights observed experimentally for supercells with lateral lengths of about 9 nm.

Field-effect devices

One of the most direct ways of accessing the electrical properties of a material is to incorporate it in an electronic device, for example in a FET (see **Figure 5**). In this multi-terminal device, current is injected by applying a voltage between source and drain electrodes, while the charge density can be modulated and the Fermi level varied using the gate electrode. FETs are not just convenient devices for probing the electrical properties of materials, but they are also the main building blocks of modern electronics, so demonstrating that a well-behaved FET can be made using a new semiconducting material is an important step in highlighting their technological relevance.

Radisavljevic et al. reported the first FET based on a 2D TMDC material in 2011.⁷ It included a HfO₂ top-gate dielectric and showed a current ON/OFF ratio exceeding 10⁸ at room temperature and OFF-state currents smaller than 25 fA/μm. For comparison, an ON/OFF ratio of 10⁶ and an OFF-state current on the order of 1 nA/μm is considered acceptable for digital electronic circuits. This showed for the first time that electronic devices with interesting performance levels could be realized based on 2D materials other than graphene. It resulted in the inclusion of MoS₂ and semiconducting TMDCs in the International Technology Roadmap for Semiconductors⁵⁵ in 2011.

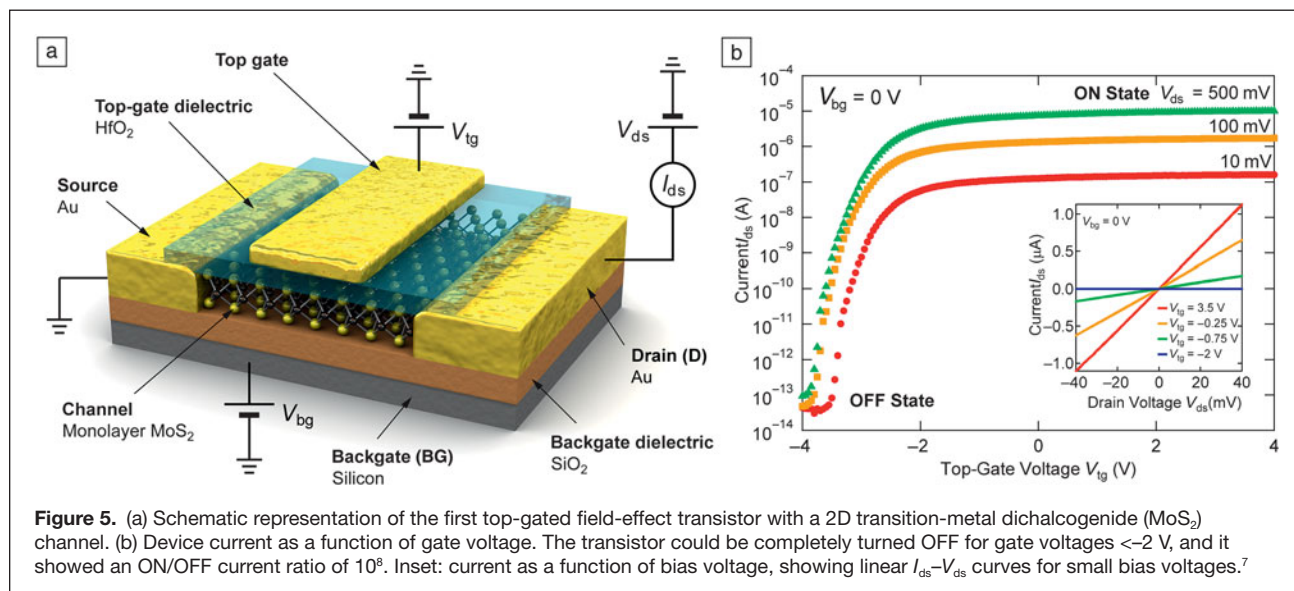
The encapsulation of MoS₂ using insulating HfO₂ was crucial in achieving high performance levels in early devices. Subsequent temperature-dependent measurements of electrical transport in various geometries⁵⁶ showed that encapsulation in HfO₂ can effectively increase the mobility of MoS₂ through a combination of homopolar phonon mode quenching^{57,58} as well as charged impurity screening by the dielectric and the top gate.⁵⁹ A complementary approach to achieving high mobility involves vacuum annealing, resulting in the removal of adsorbates,^{60,61} lower noise,⁶² and low-temperature mobilities in ML MoS₂ of ~250 cm²/Vs extracted from Hall effect measurements and

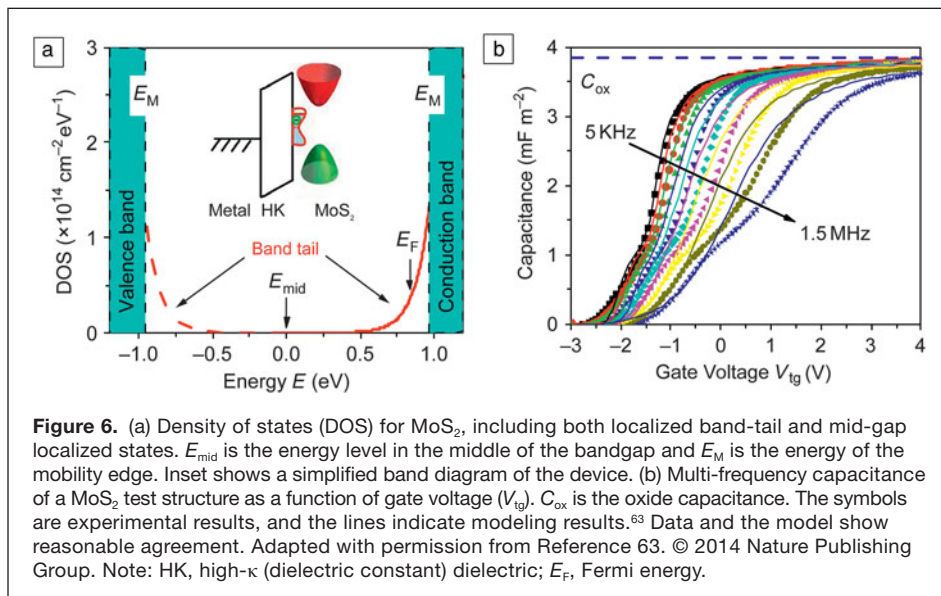
field-effect effective mobilities of ~1000 cm²/Vs.⁶¹ These values could be significantly underestimated and lower than the intrinsic limit⁵⁷ due to the presence of electronic trap states⁶³ and the formation of a band tail, as seen in **Figure 6a**. The smearing of the band edge due to various types of inhomogeneities could include sulfur vacancies, charges trapped at the TMDC/dielectric interface, or other structural defects. The extent of the band tail in MoS₂ was characterized by Zhu et al., who found a ~100 meV characteristic energy width of the band tail using frequency-dependent capacitance–voltage measurements⁶³ (**Figure 6b**).

While further increases in the mobility of MoS₂ are to be expected, it is already large enough to allow operation of MoS₂-based transistors in the GHz range, where current, voltage, and power gains were demonstrated.⁶⁴ These performance figures are mostly limited by the contact resistance.

Reducing the contact resistance due to the Schottky barrier between the 2D semiconductor and the metal and realizing an ohmic contact is one of the most important challenges for engineering a high-quality device. This is, for example, crucial in achieving highly responsive photodetectors.⁶⁵ One way to achieve this is by using low work-function metals as contacts, such as Ni⁶⁶ or Sc.^{67,68} In addition to choosing the metal with an advantageous work function, other factors such as the orbital overlap between the metals and TMDCs and the contact geometry (top versus edge contacts) also play important roles, as shown by Kang et al. first in their theoretical study⁶⁹ and later in the experimental demonstration of low-resistance Mo contacts to MoS₂.⁷⁰

A complementary approach is to reduce the Schottky barrier height by doping the semiconducting region under the contact (e.g., by *p*-doping WSe₂ devices to NO₂³¹ in order to improve Pd contacts, *n*-type doping using the chemical compound benzyl viologen to improve Ni contacts to MoS₂,⁷¹ or chlorine doping in the case of Ni on WS₂ and MoS₂).⁷²





The biggest reduction in contact resistance reported so far was by using the radical approach of converting MoS₂ in the contact region from the semiconducting 2H to the metallic 1T phase by locally increasing the charge doping level using lithiation,⁷³ resulting in a contact resistance of less than 300 $\Omega \cdot \mu\text{m}$. Previous typical contact resistance values were above 1 k $\Omega \cdot \mu\text{m}$. Not only can MoS₂ be semiconducting or metallic, but at sufficiently high doping levels, it can also become superconducting, with a gate tunable transition temperature showing a maximum at 11 K.⁷⁴

Because 2D TMDCs are direct bandgap semiconductors, FETs based on these materials can also be used as simple and efficient photodetectors. Early phototransistors based on MoS₂ had a photoresponsivity of 7.5 mA/W.⁷⁵ Using layers with different thicknesses, the responsivity of the photodetector can be tuned to different wavelength ranges.⁷⁶ Lopez-Sanchez et al.⁶⁵ reported ML MoS₂ phototransistors with a high photoresponsivity of 880 A/W.

Experimental work on other semiconducting TMDCs has also started. While MoS₂ is usually *n*-type, *p*-type FET devices based on WSe₂ have been realized showing a room-temperature hole mobility of 250 cm²/Vs³¹ as well as *n*-WSe₂ transistors with a room-temperature mobility of 142 cm²/Vs.³² Using liquid gating, in which an ionic liquid is used in place of a solid dielectric, it was possible to achieve ambipolar operation in ML WSe₂⁷⁷ as well as in WS₂.⁷⁸

While most of the work in 2D TMDC-based transistors has focused on using a 2D material as the semiconducting channel, the wide range of electrical properties represented by 2D materials, from insulating such as boron nitride (BN) to superconducting, implies

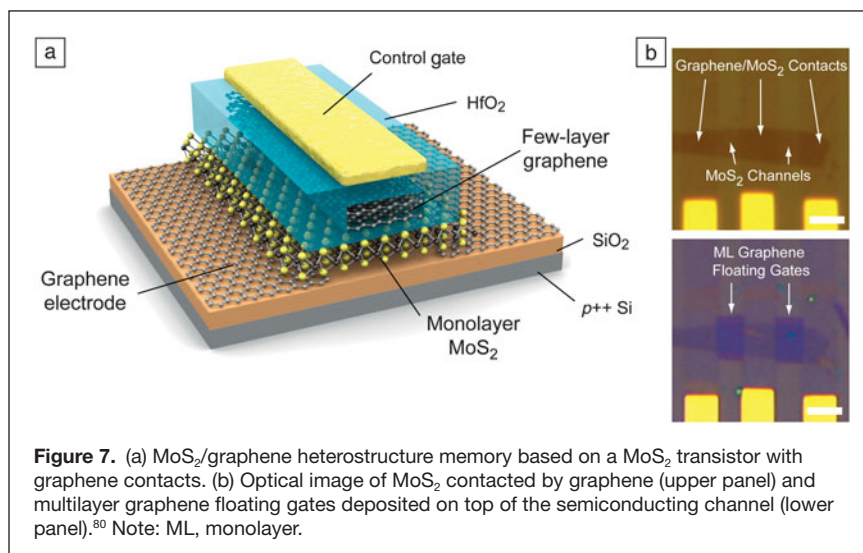
that, in principle, all parts of an FET structure can be replaced by 2D materials. The lack of dangling bonds in 2D materials also weakens the usual constraints of lattice matching that limit the possible combinations for “classical” three-dimensional materials. This allows for the realization of a host of new types of devices, such as vertical FETs with several BN¹² or TMDC layers⁷⁹ sandwiched between graphene electrodes.

Being a good conductor, graphene can be used as an electrical contact for lateral electrical transport through MoS₂ and other 2D semiconductors. Bertolazzi et al.⁸⁰ demonstrated flash memory cells based on ML MoS₂ contacted by low-resistance ohmic-like graphene contacts (see **Figure 7**).

By using BN as the gate insulator, the entire FET structure could be implemented using 2D materials as the contact, semiconducting channel, and gate insulator.⁸¹

Electronic circuits

Electronic circuits based on 2D TMDC semiconductors have already been demonstrated. Radisavljevic et al.⁸² realized the first such circuit, which consisted of two transistors on the same piece of ML MoS₂ and operating as an inverter. The gain of the inverter was higher than 4, indicating that such logic gates could be integrated into more complicated circuits without attenuation of voltage levels. The same device can also be operated as an analogue amplifier⁸³ for small signals. Logic circuits based on BL MoS₂⁸⁴ and complementary inverters based on WSe₂⁸⁵ were also demonstrated, as were ring oscillators and random access memory circuits.⁸⁴ Bertolazzi et al.⁸⁰ demonstrated flash memory cells, with operating principles similar to



the ones used in consumer electronic devices such as cell phones and cameras, in a heterostructure geometry. Such devices could offer reduced crosstalk between neighboring memory cells and could be scaled to smaller sizes due to the high sensitivity of the ML MoS₂ semiconducting channel to the charge stored on the multilayer graphene floating gate.

Flexible devices

In addition to its interesting electronic applications, TMDC semiconductors have favorable mechanical properties. The first mechanical measurements of the stiffness and breaking strength of single and BL MoS₂ were carried out by suspending MoS₂ membranes on perforated substrates and deforming them using an AFM tip.⁸⁶ These experiments showed that MoS₂ has a Young's modulus of ~270 GPa, higher than that of steel (~205 GPa). The breaking strength of single and BL MoS₂ was between 6% and 11% of their respective Young's modulus, which represents the upper theoretical limit of a material's breaking strength⁸⁷ and reflects the intrinsic properties of its interatomic bonds. This makes ML MoS₂ the strongest semiconducting material and suggests that MoS₂ is suitable for integration with flexible plastic substrates, such as polyimide, whose maximum strain before failure is ~7%. Similar mechanical properties are expected in all TMDC materials because of the similar nature of interatomic bonds in these materials. Therefore, MoS₂ is an interesting material for flexible electronics and nanoelectromechanical systems. Castellanos-Gomez et al.⁸⁸ realized the first devices of this kind when they demonstrated nanomechanical resonators based on ML MoS₂ membranes with resonant frequencies of up to 30 MHz. A number of flexible FETs based on MoS₂ have been realized using liquid gels,⁸⁹ high- κ (where κ is the dielectric constant),⁹⁰ or BN⁹¹ as dielectrics, and show robust electrical operation against mechanical deformation.

Summary

We have summarized the most recent work on MoS₂ and other Group 6 TMDC materials, focusing on their electronic properties and their potential to enter the field of next-generation 2D electronics, including applications in low-power electronics (due to reduction of leakage currents and contact resistance), flexible electronics, optoelectronics, and straintronics. The enormous progress of the field, ranging from fundamental science up to device implementation, is reflected by the large number of scientists working in the field, even though the first transistor on a MoS₂ ML was reported only recently. MoS₂ and other TMDCs are being developed, in synergy with graphene and hexagonal boron nitride, as important material components for 2D electronics. The work has just begun, and a large number of TMDCs have not even been synthesized or studied.

Acknowledgments

This work was financially supported by the European Research Council (grants no. 240076 & no. 256962), Marie

Curie ITN network "MoWSeS" (grant no. 317451), the Swiss National Science Foundation (grants no. 132102 and 138237), Swiss SNF Sinergia Grant no. 147607, and Deutsche Forschungsgemeinschaft (HE 3543/19–1).

References

1. A. Kuc, T. Heine, *Chem. Soc. Rev.* (2014), doi, 10.1039/C4CS00276H.
2. Q.H. Wang, K. Kalantar-Zadeh, A. Kis, J.N. Coleman, M.S. Strano, *Nat. Nanotechnol.* **7**, 699 (2012).
3. K.S. Novoselov, A.K. Geim, S.V. Morozov, D. Jiang, Y. Zhang, S.V. Dubonos, I.V. Grigorieva, A.A. Firsov, *Science* **306**, 666 (2004).
4. K.S. Novoselov, *Rev. Mod. Phys.* **83**, 837 (2011).
5. Y. Zhang, T.-T. Tang, C. Girit, Z. Hao, M.C. Martin, A. Zettl, M.F. Crommie, Y.R. Shen, F. Wang, *Nature* **459**, 820 (2009).
6. F. Xia, D.B. Farmer, Y. Lin, P. Avouris, *Nano Lett.* **10**, 715 (2010).
7. B. Radisavljevic, A. Radenovic, J. Brivio, V. Giacometti, A. Kis, *Nat. Nanotechnol.* **6**, 147 (2011).
8. F. Wypych, R. Schollhorn, *J. Chem. Soc. Chem. Commun.* **19**, 1386 (1992).
9. K.S. Novoselov, D. Jiang, F. Schedin, T.J. Booth, V.V. Khotkevich, S.V. Morozov, A.K. Geim, *Proc. Natl. Acad. Sci. U.S.A.* **102**, 10451 (2005).
10. M.M. Benameur, B. Radisavljevic, J.S. Heron, S. Sahoo, H. Berger, A. Kis, *Nanotechnology* **22**, 125706 (2011).
11. J.N. Coleman, M. Lotya, A. O'Neill, S.D. Bergin, P.J. King, U. Khan, K. Young, A. Gaucher, S. De, R.J. Smith, I.V. Shvets, S.K. Arora, G. Stanton, H.Y. Kim, K. Lee, G.T. Kim, G.S. Duesberg, T. Hallam, J.J. Boland, J.J. Wang, J.F. Donegan, J.C. Grunlan, G. Moriarty, A. Shmeliov, R.J. Nicholls, J.M. Perkins, E.M. Grievson, K. Theuwissen, D.W. McComb, P.D. Nellist, V. Nicolosi, *Science* **331**, 568 (2011).
12. S. Najmaei, Z. Liu, W. Zhou, X. Zou, G. Shi, S. Lei, B.I. Yakobson, J.-C. Idrobo, P.M. Ajayan, J. Lou, *Nat. Mater.* **12**, 754 (2013).
13. A.M. van der Zande, P.Y. Huang, D.A. Chenet, T.C. Berkelbach, Y. You, G.-H. Lee, T.F. Heinz, D.R. Reichman, D.A. Muller, J.C. Hone, *Nat. Mater.* **12**, 554 (2013).
14. L. Britnell, R.V. Gorbachev, R. Jalil, B.D. Belle, F. Schedin, A. Mishchenko, T. Georgiou, M.I. Katsnelson, L. Eaves, S.V. Morozov, N.M.R. Peres, J. Leist, A.K. Geim, K.S. Novoselov, L.A. Ponomarenko, *Science* **335**, 947 (2012).
15. J.A. Wilson, A.D. Yoffe, *Adv. Phys.* **18**, 193 (1969).
16. R.F. Frindt, A.D. Yoffe, *Proc. R. Soc. Lond. A* **273**, 69 (1963).
17. P. Joensen, R.F. Frindt, S.R. Morrison, *Mater. Res. Bull.* **21**, 457 (1986).
18. K.K. Kam, B.A. Parkinson, *J. Phys. Chem.* **86**, 463 (1982).
19. A. Splendiani, L. Sun, Y. Zhang, T. Li, J. Kim, C.-Y. Chim, G. Galli, F. Wang, *Nano Lett.* **10**, 1271 (2010).
20. K.F. Mak, C. Lee, J. Hone, J. Shan, T.F. Heinz, *Phys. Rev. Lett.* **105**, 136805 (2010).
21. A. Kuc, N. Zibouche, T. Heine, *Phys. Rev. B Condens. Matter* **83**, 245213 (2011).
22. T. Li, G. Galli, *J. Phys. Chem. C* **111**, 16192 (2007).
23. L. Liu, S.B. Kumar, Y. Ouyang, J. Guo, *IEEE Trans. Electron Devices* **58**, 3042 (2011).
24. Y. Ding, Y. Wang, J. Ni, L. Shi, S. Shi, W. Tang, *Physica B* **406**, 2254 (2011).
25. C. Ataca, H. Şahin, S. Ciraci, *J. Phys. Chem. C* **116**, 8983 (2012).
26. *Acc. Chem. Res.* **48**, 1 (2015).
27. N.E. Staley, J. Wu, P. Eklund, Y. Liu, L. Li, Z. Xu, *Phys. Rev. B Condens. Matter* **80**, 184505 (2009).
28. M.N. Ali, J. Xiong, S. Flynn, J. Tao, Q.D. Gibson, L.M. Schoop, T. Liang, N. Haldolaarachchige, M. Hirschberger, N.P. Ong, R.J. Cava, *Nature* **514**, 205 (2014).
29. S. Tongay, J. Zhou, C. Ataca, K. Lo, T.S. Matthews, J. Li, J.C. Grossman, J. Wu, *Nano Lett.* **12**, 5576 (2012).
30. W.S. Hwang, M. Remskar, R. Yan, V. Protasenko, K. Tahy, S.D. Chae, P. Zhao, A. Konar, H. Xing, A. Seabaugh, D. Jena, *Appl. Phys. Lett.* **101**, 013107 (2012).
31. H. Fang, S. Chuang, T.C. Chang, K. Takei, T. Takahashi, A. Javey, *Nano Lett.* **12**, 3788 (2012).
32. W. Liu, J. Kang, D. Sarkar, Y. Khatami, D. Jena, K. Banerjee, *Nano Lett.* **13**, 1983 (2013).
33. P. Miró, M. Audiffred, T. Heine, *Chem. Soc. Rev.* **43**, 6537 (2014).
34. S. Tongay, H. Şahin, C. Ko, A. Luce, W. Fan, K. Liu, J. Zhou, Y.-S. Huang, C.-H. Ho, J. Yan, D.F. Ogletree, S. Aloni, J. Ji, S. Li, J. Li, F.M. Peeters, J. Wu., *Nat. Commun.* **5**, 3252 (2014).
35. S. Yang, S. Tongay, Q. Yue, Y. Li, B. Li, F. Lu, *Sci. Rep.* **4**, 5442 (2014).
36. T. Heine, *Acc. Chem. Res.* **48**, 65 (2015).
37. P. Miro, M. Audiffred, T. Heine, *Chem. Soc. Rev.* **43**, 6537 (2014).
38. P. Miro, M. Ghorbani-Asl, T. Heine, *Angew. Chem. Int. Ed.* **53**, 3015 (2014).
39. Z.Y. Zhu, Y.C. Cheng, U. Schwingenschlögl, *Phys. Rev. B Condens. Matter* **84**, 153402 (2011).
40. N. Zibouche, A. Kuc, J. Musfeldt, T. Heine, *Ann. Phys.* **526**, 395 (2014).

41. N. Zibouche, P. Philipsen, A. Kuc, T. Heine, *Phys. Rev. B Condens. Matter* **90**, 125440 (2014).
42. N. Zibouche, P. Philipsen, T. Heine, A. Kuc, *Phys. Chem. Chem. Phys.* **16**, 11251 (2014).
43. I. Kaplan-Ashiri, S.R. Cohen, K. Gartsman, V. Ivanovskaya, T. Heine, G. Seifert, I. Wiesel, H.D. Wagner, R. Tenne, *Proc. Natl. Acad. Sci. U.S.A.* **103**, 523 (2006).
44. M. Ghorbani-Asl, S. Borini, A. Kuc, T. Heine, *Phys. Rev. B Condens. Matter* **87**, 235434 (2013).
45. M. Ghorbani-Asl, N. Zibouche, M. Wahiduzzaman, A.F. Oliveira, A. Kuc, T. Heine, *Sci. Rep.* **3**, 2961, (2013).
46. T. Lorenz, M. Ghorbani-Asl, J.-O. Joswig, T. Heine, G. Seifert, *Nanotechnology* **25**, 445201 (2014).
47. G. Plechinger, A. Castellanos-Gomez, M. Buscema, H. van der Zant, G. Steele, A. Kuc, T. Heine, C. Schüller, T. Korn, *2D Mater.* (2015) (forthcoming).
48. K. He, C. Poole, K.F. Mak, J. Shan, *Nano Lett.* **13**, 2931 (2013).
49. H.J. Conley, B. Wang, J.I. Ziegler, R.F. Haglund, S.T. Pantelides, K.I. Bolotin, *Nano Lett.* **13**, 3626 (2013).
50. S. Tongay, J. Suh, C. Ataca, W. Fan, A. Luce, J.S. Kang, J. Liu, C. Ko, R. Raghunathanan, J. Zhou, F. Ogletree, J. Li, J.C. Grossman, J. Wu, *Sci. Rep.* **3**, 2657, (2013).
51. M. Ghorbani-Asl, A.N. Enyashin, A. Kuc, G. Seifert, T. Heine, *Phys. Rev. B Condens. Matter* **88**, 245440 (2013).
52. H. Qiu, T. Xu, Z. Wang, W. Ren, H. Nan, Z. Ni, Q. Chen, S. Yuan, F. Miao, F. Song, G. Long, Y. Shi, L. Sun, J. Wang, X. Wang, *Nat. Commun.* **4**, 2642, (2013).
53. J. Brivio, D.T.L. Alexander, A. Kis, *Nano Lett.* **11**, 5148 (2011).
54. P. Miro, M. Ghorbani-Asl, T. Heine, *Adv. Mater.* **25**, 5473 (2013).
55. International Technology Roadmap for Semiconductors (2011), <http://www.itrs.net/>.
56. B. Radisavljevic, A. Kis, *Nat. Mater.* **12**, 815 (2013).
57. K. Kaasbjerg, K.S. Thygesen, K.W. Jacobsen, *Phys. Rev. B Condens. Matter* **85**, 115317 (2012).
58. K. Kaasbjerg, K.S. Thygesen, A.-P. Jauho, *Phys. Rev. B Condens. Matter* **87**, 235312 (2013).
59. Z.-Y. Ong, M.V. Fischetti, *Phys. Rev. B Condens. Matter* **88**, 165316 (2013).
60. D. Jariwala, V.K. Sangwan, D.J. Late, J.E. Johns, V.P. Dravid, T.J. Marks, L.J. Lauhon, M.C. Hersam, *Appl. Phys. Lett.* **102**, 173107 (2013).
61. B. Baugher, H.O.H. Churchill, Y. Yang, P. Jarillo-Herrero, *Nano Lett.* **13**, 4212 (2013).
62. X. Xie, D. Sarkar, W. Liu, J. Kang, O. Marinov, M.J. Deen, K. Banerjee, *ACS Nano* **8**, 5633 (2014).
63. W. Zhu, T. Low, Y.-H. Lee, H. Wang, D.B. Farmer, J. Kong, F. Xia, P. Avouris, *Nat. Commun.* **5**, 3087 (2014).
64. D. Krasnozhan, D. Lembke, C. Nyffeler, Y. Leblebici, A. Kis, *Nano Lett.* **14**, 5905 (2014).
65. O. Lopez-Sanchez, D. Lembke, M. Kayci, A. Radenovic, A. Kis, *Nat. Nanotechnol.* **8**, 497 (2013).
66. A.T. Neal, H. Liu, J.J. Gu, P.D. Ye, *Proc. 2012 70th Ann. Dev. Res. Conf. (DRC)* (2012), p. 65.
67. I. Popov, G. Seifert, D. Tománek, *Phys. Rev. Lett.* **108**, 156802 (2012).
68. S. Das, H.-Y. Chen, A.V. Penumatcha, J. Appenzeller, *Nano Lett.* **13**, 100 (2013).
69. J. Kang, W. Liu, D. Sarkar, D. Jena, K. Banerjee, *Phys. Rev. X* **4**, 031005 (2014).
70. J. Kang, W. Liu, K. Banerjee, *Appl. Phys. Lett.* **104**, 233502 (2014).
71. D. Kiriya, M. Tosun, P. Zhao, J.S. Kang, A. Javey, *J. Am. Chem. Soc.* **136**, 7853 (2014).
72. L. Yang, K. Majumdar, H. Liu, Y. Du, H. Wu, M. Hatzistergos, P.Y. Hung, R. Tieckelmann, W. Tsai, C. Hobbs, P.D. Ye, *Nano Lett.* (2014), available at <http://arxiv.org/pdf/1410.8201>.
73. R. Kappera, D. Voiry, S.E. Yalcin, B. Branch, G. Gupta, A.D. Mohite, M. Chhowalla, *Nat. Mater.* **13**, 1128 (2014).
74. J.T. Ye, Y.J. Zhang, R. Akashi, M.S. Bahramy, R. Arita, Y. Iwasa, *Science* **338**, 1193 (2012).
75. Z. Yin, H. Li, H. Li, L. Jiang, Y. Shi, Y. Sun, G. Lu, Q. Zhang, X. Chen, H. Zhang, *ACS Nano* **6**, 74 (2012).
76. H.S. Lee, S.-W. Min, Y.-G. Chang, M.K. Park, T. Nam, H. Kim, J.H. Kim, S. Ryu, S. Im, *Nano Lett.* **12**, 3695 (2012).
77. A. Allain, A. Kis, *ACS Nano* **8**, 7180 (2014).
78. S. Jo, N. Ubrig, H. Berger, A.B. Kuzmenko, A.F. Morpurgo, *Nano Lett.* **14**, 2019 (2014).
79. T. Georgiou, R. Jalil, B.D. Belle, L. Britnell, R.V. Gorbachev, S.V. Morozov, Y.-J. Kim, A. Gholinia, S.J. Haigh, O. Makarovskiy, L. Eaves, L.A. Ponomarenko, A.K. Geim, K.S. Novoselov, A. Mishchenko, *Nat. Nanotechnol.* **8**, 100 (2013).
80. S. Bertolazzi, D. Krasnozhan, A. Kis, *ACS Nano* **7**, 3246 (2013).
81. T. Roy, M. Tosun, J.S. Kang, A.B. Sachid, S.B. Desai, M. Hettick, C.C. Hu, A. Javey, *ACS Nano* **8**, 6259 (2014).
82. B. Radisavljevic, M.B. Whitwick, A. Kis, *ACS Nano* **5**, 9934 (2011).
83. B. Radisavljevic, M.B. Whitwick, A. Kis, *Appl. Phys. Lett.* **101**, 043103 (2012).
84. H. Wang, L. Yu, Y.-H. Lee, Y. Shi, A. Hsu, M.L. Chin, L.-J. Li, M. Dubey, J. Kong, T. Palacios, *Nano Lett.* **12**, 4674 (2012).
85. M. Tosun, S. Chuang, H. Fang, A.B. Sachid, M. Hettick, Y. Lin, Y. Zeng, A. Javey, *ACS Nano* **8**, 4948 (2014).
86. S. Bertolazzi, J. Brivio, A. Kis, *ACS Nano* **5**, 9703 (2011).
87. A. Griffith, *Philos. Trans. R. Soc. Lond. A* **221**, 163 (1920).
88. A. Castellanos-Gomez, R. van Leeuwen, M. Buscema, H.S.J. van der Zant, G.A. Steele, W.J. Venstra, *Adv. Mater.* **25**, 6719 (2013).
89. J. Pu, Y. Yomogida, K.-K. Liu, L.-J. Li, Y. Iwasa, T. Takenobu, *Nano Lett.* **12**, 4013 (2012).
90. H.-Y. Chang, S. Yang, J. Lee, L. Tao, W.-S. Hwang, D. Jena, N. Lu, D. Akinwande, *ACS Nano* **7**, 5446 (2013).
91. G.-H. Lee Y.-J. Yu, X. Cui, N. Petrone, C.-H. Lee, M.S. Choi, D.-Y. Lee, C. Lee, W.J. Yoo, K. Watanabe, T. Taniguchi, C. Nuckolls, P. Kim, J. Hone, *ACS Nano* **7**, 7931 (2013). □



MRS MATERIALS RESEARCH SOCIETY®
Advancing materials. Improving the quality of life.

JOIN OR **RENEW** YOUR MRS MEMBERSHIP TODAY!

NEW MEMBERSHIP BENEFIT Adding to the many core benefits MRS membership offers, **effective July 1, 2015**, MRS members will receive a FREE electronic subscription to *Journal of Materials Research (JMR)*—access to full-text articles from the *Journal's* inception in January 1986 to the current issue.

Visit WWW.MRS.ORG/MEMBERSHIP for a complete list of MRS member benefits.